INSTITUT DE FRANCE
Académie des sciences

Comptes Rendus

Physique

Alain Lecavelier des Etangs

Evaporation, from exoplanets to exocomets

Published online: 8 June 2023

https://doi.org/10.5802/crphys.142

Part of Special Issue: Exoplanets
Guest editors: Anne-Marie Lagrange (LESIA, Observatoire de Paris, Université PSL, CNRS, Sorbonne Université, Sorbonne Paris Cité, 5 place Jules Janssen, 92195 Meudon, France.) and Daniel Rouan (LESIA, Observatoire de Paris, Université PSL, CNRS, Sorbonne Université, Sorbonne Paris Cité, 5 place Jules Janssen, 92195 Meudon, France.)

CENTRE MERSENNE

Les Comptes Rendus. Physique *sont membres du Centre Mersenne pour l'édition scientifique ouverte*
www.centre-mersenne.org
e-ISSN : 1878-1535

Comptes Rendus
Physique
Published online: 8 June 2023
https://doi.org/10.5802/crphys.142

Exoplanets / *Exoplanètes*

Evaporation, from exoplanets to exocomets

Évaporation, des exoplanètes aux exocomètes

Alain Lecavelier des Etangs*, [a]

[a] Institut d'astrophysique de Paris, CNRS, UMR 7095, Sorbonne Université, Paris, France
E-mail: lecaveli@iap.fr

Abstract. Here we review the last advances in our understanding of exoplanetary upper atmospheres, with a focus on the evaporation of exoplanets orbiting close to their stars. The atmospheric escape takes a significant part on the phenomena that sculpt the population of planets with short orbital distances.

We also observe evaporation of minor bodies in young planetary systems when they approach to their star. These "exocomets" have been studied since the mid 80's, yielding a large amount of observational data. In particular, in the case of exocomets orbiting the young star β Pictoris, it has been shown that there are two different families of comets, tracing two different dynamical histories. Most recently, photometric observations with the NASA TESS space observatory allowed the detection of the dust tails produced by the evaporation of the exocomets' nuclei. Using numerical simulation these observations allowed the derivation of the comets nuclei size distribution, which is found to be strikingly similar to the one observed in the Solar system and to the one expected for a collisionally relaxed population of minor bodies.

Résumé. Une énorme quantité de travaux observationnels et théoriques ont été réalisés pour comprendre la physique et la chimie de la petite couche de gaz entourant les exoplanètes que l'on désigne aussi par le terme « atmosphère ». Avec l'aide d'observatoires spatiaux comme le télescope spatial Hubble ou l'observatoire infrarouge Spitzer, ou avec les derniers spectrographes au foyer des plus grands télescopes au sol, les données collectées sont aujourd'hui extrêmement riches en informations. La principale conclusion de ces vingt dernières années d'observations d'atmosphères d'exoplanètes est l'étonnante diversité des planètes qui ont été découvertes.

Nous nous intéressons ici à un phénomène particulier : l'évaporation d'exoplanètes qui sont en orbite très près de leurs étoiles. Nous décrivons les observations de l'échappement atmosphérique des exoplanètes. Puis nous montrerons les conséquences de ce phénomène sur les propriétés physiques des exoplanètes. Nous montrons que l'évaporation de petits corps est également observée dans certains systèmes extrasolaires, conduisant à la découverte d'exocomètes. Les observations spectroscopiques et photométriques ont permis de scruter les composantes de gaz et de poussières des queues cométaires. Enfin, les observations photométriques détaillées des exocomètes ont permis de mesurer les tailles des noyaux de comètes dans le système planétaire de β Pictoris ; la distribution de taille observée montre l'importance des collisions dans les dernières étapes de la formation des systèmes planétaires.

Keywords. Exoplanets, Atmospheres, Exocomets, Planetary systems, Circumstellar disks, Atmospheric escape, Beta Pictoris.

Mots-clés. Exoplanètes, Atmosphères, Exocomètes, Systèmes planétaires, Disques circumstellaires, Échappement atmosphérique, Bêta Pictoris.

* Corresponding author.

Note. Follows up on a conference-debate of the French Academy of Sciences entitled “Exoplanets: the new challenges” held on 18May 2021, visible via
https://www.academie-sciences.fr/fr/Colloques-conferences-et-debats/exoplanetes.html..
Note. Fait suite à une conférence-débat de l’Académie des sciences intitulée “ Exoplanètes : les nouveaux défis” tenue le 18 mai 2021, visible via
https://www.academie-sciences.fr/fr/Colloques-conferences-et-debats/exoplanetes.html..
Published online: 8 June 2023

1. Introduction

This paper does not pretend to be an exhaustive review on the exoplanets atmospheres. Indeed, since the first observations of exoplanets atmospheres twenty years ago [1, 2], a huge amount of observational and theoretical works has been made to understand the physics and the chemistry of the small layers of gas surrounding the discovered exoplanets, the so-called atmospheres. With the help of space observatories like the Hubble space telescope or the Spitzer infrared observatory, or with the latest spectrographs on the largest ground-based telescopes, the collected data are nowadays extremely rich in information. The main conclusion of these last twenty years of exoplanets atmospheres observations is the amazing diversity of planets that have been discovered (see, e.g., [3]).

Here we will focus on a peculiar phenomenon: the evaporation of exoplanets orbiting close to their stars. In the first part of the paper, we will describe the observations of the exoplanets atmospheric escape. Then we will show the consequences of this main phenomenon on the physical properties of the exoplanets. In the following section, we will show that evaporation of minor bodies is also observed in extrasolar systems, leading to the discoveries of exocomets. The spectroscopic and photometric observations allowed to scrutinize the gaseous and the dusty component of the cometary tails. Finally, the detailed photometric observations of exocomets allowed to derive the sizes of comets nuclei in the β Pictoris planetary system; the observed size distribution points towards the importance of collisions in the final stages of planetary systems formation.

2. Exoplanets atmospheres

There are several methods to detect the atmosphere of an exoplanet. The most obvious one, the direct observation of the planet, is also certainly the most challenging because of the need to cancel the stellar light to obtain a spectrum of the planet itself. This can be done with the most advanced adaptive optics and coronographic technologies. However, the number of direct detections remains limited to a few cases.

For now, the most detailed and numerous observations of exoplanets atmospheres have been obtained using the transit technique. When the axis of the planet’s orbit in nearly perpendicular to the line of sight from the Earth to the star, at each orbit the planet passes in front of and behind the star. When the planet is seen in front of the star, a small fraction of the stellar light goes trough the atmosphere that imprints its signature into the observed spectrum. When the planet passes behind the star, its emitted and reflected light is eclipsed by the star; therefore it is possible to deduce the properties of the planetary light by measuring the difference between the light received when the planet is not eclipsed and when the planet is eclipsed.

One interesting example of an exoplanet’s upper atmosphere observation using eclipse observations has been performed using the Hubble space telescope in the infrared, at wavelengths where the thermal emission from the hot planet WASP-121 b is large enough to be disentangled from the star light by comparison of the spectrum obtained during and after the eclipse [4]. In the spectroscopic band of water around 1.4μm, the planet was expected to be less bright than at nearby wavelengths, producing an absorption signature in the spectrum. Indeed, the presence of water makes the atmosphere opaque at ~1.4μm, and the measured thermal emission is thus coming from higher altitudes than the emission at other wavelengths where the atmosphere is more transparent. At higher altitude the atmosphere was expected to be cooler, meaning lower thermal emission. However the observations revealed an emission feature with a planet brighter at 1.4μm than at 1.3 or 1.6μm, showing a surprising inverted thermal profile with higher temperatures at higher altitude in the stratosphere.

Using transit observations a large amount of various species have been detected in a large number of exoplanets. The observation of water in the atmosphere of the planet K2-18 b is an example of a recent discovery that grabbed attention, in particular because this concerns a low mass planet (8 Earth mass) that is located in the habitable zone suggesting the possibility to have a fraction of liquid water [5, 6]. This discovery triggered significant efforts of modeling for a better understanding of the circulation of the atmosphere in 3D and the possible condensation of water at the limb of the planet [7]. However, it remains possible that the absorption was not that of water but of methane [8], showing the difficulty of such observations and of their interpretation. Whether it is water or methane, this shows the richness of this transit technique that will be even more powerful with the commissioning of the new James Webb Space Telescope (JWST).

To conclude on the transit technique, it should be emphasized that this technique is not limited only to the detection of the atmosphere chemical constituents, but also allows the measurements of physical properties. To do this, we take advantage of the fact that, in contrary to the emission spectrum, the transit absorption spectrum of the planet atmosphere does not depend upon the temperature-pressure vertical profile of the atmosphere [9]. Among the measured physical quantities, one can cite the temperature [10], the pressure [11], the variation of the temperature with the altitude in the atmosphere [12, 13], the mean molecular mass [14], and even the atmosphere rotation rate and the wind velocity at the limb in the planet β Pictoris [15].

3. Evaporation of exoplanets

When a planet is close to its host-star, like 51 Peg b [16], the upper atmosphere is heated by the X-ray and EUV stellar radiation [17]. This energy can be used by the atmosphere to escape the gravitational potential well leading to the atmospheric escape or evaporation. The first detection of an exoplanet evaporation has been made for the planet HD209458 b using transit spectroscopy in Lyman-α with the Hubble space telescope [2] (Fig. 1).

For HD209458 b the escape rate is estimated to be around $10^{10}\,\mathrm{g\,s^{-1}}$, which is not that high. With a total mass of 0.69 Jupiter mass, the atmospheric evaporation does not significantly affect the interior structure or the nature of the planet. However, for lower mass planets the situation is different. For instance, for GJ436b the transit in front of the star yields a Lyman-α absorption of about 50% showing that the escaping gas produces a giant exosphere about half the size of the star [19]. In this case, the derived escape rate corresponds to a mass loss of about 10% of the planet mass during the system life [20–22]. The situation is even more striking in the case of the Neptune mass planet GJ3470b. For this planet the observation of the evaporation in Lyman-α yields an escape rate of about $10^{10}\,\mathrm{g\,s^{-1}}$ and models indicate that the planet can loose up to 35% of its current mass over its two billion years lifetime [23].

For Neptune mass planets, a large evaporation rate can lead to a change in the planetary nature, transforming a planet with a massive gaseous envelope into a rocky planet devoid of a thick atmosphere [24–27]. For instance, the evaporation is certainly the key for understanding

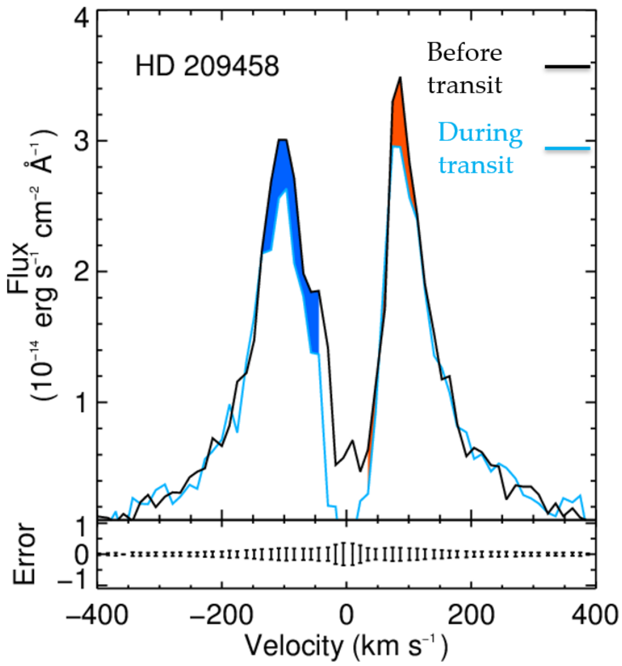

Figure 1. Lyman-α spectrum of HD209458 before and during the transit (black and blue lines, respectively). The escaping atomic hydrogen produces an absorption of about 10 to 15% showing that the gas is well beyond the Roche lobe of the planet. The gas velocity also reaches -130 km $^{-1}$, that is beyond the planet's escape velocity of about 50 km $^{-1}$. These two properties show that the planet is evaporating [2, 18].
(Courtesy of V. Bourrier).

the amazing large density contrast between the two planets Kepler-36 b and Kepler-36 c although they orbit the same star and have similar masses [28]. Here this difference between the two planets is explained by the difference in mass loss history due to the difference in the masses of the planets' rock/iron cores and the impact that this has on the mass-loss evolution.

In conclusion, the unexpected discovery of significant evaporation of exoplanets close to their star provides a key to understand some aspects of the planetary system diversity. Over time up to billion of years, Neptune like planets with large H/He envelopes can be transformed into rocky super-Earths. The evaporation impacts significantly the nature of the observed planets, well after the planet formation period.

4. Exocomets

The discovery of the evaporation from exoplanets shows that the key feature of the detections is the presence of extended gaseous envelopes around the planets that are detected through their absorption signature in transit observations. The size of the parent bodies does not matter; what matters is the size of the clouds of the escaping material surrounding the evaporating bodies. This explains why, although comets nuclei are only kilometer-sized bodies, they can be detected through the observations of their dust and gaseous tails when they transit in front of their host-star. In spectroscopy, we can detect the gaseous component of the cometary tails. In photometry, we can detect the transit of the dust component of the tails.

4.1. *Spectroscopy*

The first detections of exocomets have been done well before the first detections of exoplanets. In the mid eighties, the Alfred Vidal-Madjar's team, including Roger Ferlet, Anne-Marie Lagrange and Hervé Beust, noticed significant variations on short time scales in the spectrum of the young star β Pictoris, first in the lines of Ca II, and subsequently in many other lines, including for instance Fe II, Mg II and Al III. They rapidly proposed that this phenomenon can be interpreted by the transit of small evaporating bodies, that is exocomets [29]. This interpretation is now well supported by detailed models ([30, 31]) and observations (see, e.g., [32, 33]).

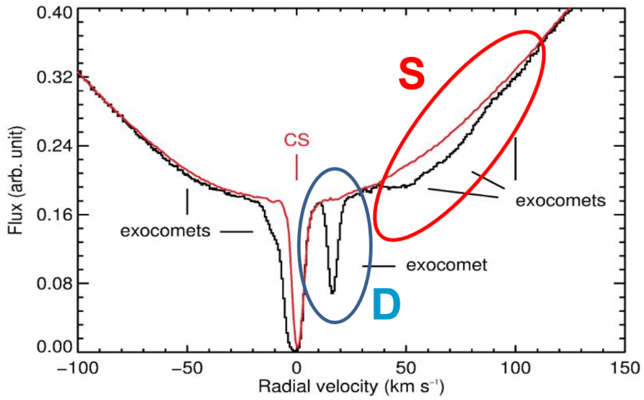

Figure 2. Ca II spectrum of β Pictoris showing the transit of several exocomets. The stellar spectrum without transiting comets is shown with a red line. The differences between the observed spectrum (black line) and the reference stellar spectrum are absorptions caused by the gaseous component of exocomets transiting in front of the star. The deep and shallow absorptions are due to comets belonging to the "D" and "S" family, respectively. (From [34], courtesy of F. Kiefer)

Even more, the analysis of several years of observations collected with the *HARPS* spectrograph at the 3.6m ESO telescope yields the detection of almost 500 exocomets in spectroscopy [34]. A statistical analysis of these large sample of exocomets, including measurements of the radial velocity thanks to the Doppler effect of the observed Ca II doublet, allowed to show the presence of two different families of exocomets orbiting β Pictoris [34]: (1) a family of old comets producing shallow absorptions ("S" family) whose orbital properties can be explained by a mean motion resonance with a massive planet, possibly β Pic b [31], and (2) a family of young comets producing deep absorptions ("D" family) with all the same periastron distance and periastron longitude. This last family of bodies with high evaporation efficiency can be the result of the break-up of a single larger parent body, *à la* Shoemeker–Levy-9 (Fig. 2). Of course that larger body could also originate from the same resonant process as the other family and have been broken by tides at its periastron passage when its periastron distance were too small.

Using spectroscopy, exocomets have been also detected orbiting stars other than β Pictoris. For instance, survey in the Ca II lines allowed to identify several exocomets transiting in front of the young star HD172555 [35]. The presence of transiting exocomets has been later confirmed by Hubble observations [36]. With UV spectra of HD172555 taken at two different epochs, Grady et al. detected variable absorption signatures of high velocity gas in the spectral lines of highly ionized species (Si III, Si IV, C IV), together with single ionized carbon and neutral atomic oxygen. These variable features are interpreted by the passage of star-grazing comets in front of the star in this young planetary system.

The discovery of exocomets of 49 Cet follows a similar story: transiting star-grazing exocomets were indeed detected on close-in orbits in the optical as variable absorptions in the Ca II lines [37]. The exocomets transit scenario was then confirmed by UV observations of carbon lines (C II and C IV) using the Hubble space telescope [38, 39].

Other young A-type stars show spectroscopic variations that can be interpreted as due to exocomets transits : HR10 [40], 51 Ophiuchi [41], HR 2174 [42], 5 Vulpeculae [37, 43], 2 Andromedae [37], HD 21620 [44], HD 110411 [44], HD 145964 [44], HD 183324 [44]. However all these detections deserve to be confirmed by other independent observations.

4.2. *Photometry*

The photometry allows the measurement of the star light dimming when a cometary dust tail passes in transit in front of its star. The major difficulty is that the decrease of the star brightness during the transit has an amplitude of about 10^{-3} to 10^{-4}, which needs space-born high accuracy photometric capabilities to be detected and measured. These capabilities have been achieved with the two NASA missions Kepler and TESS.

The shape of an exocomet transit light curve (the curve of the star brightness as a function of time) has been predicted more than twenty years ago [45, 46], but such transits have been detected only recently. The first detections have been made using Kepler observations. Exocomets transits have been proposed to explain the photometric variations of the very peculiar star KIC 8462852 [47]. In particular, the same photometric event took place twice, 928 days apart. A drop in the star brightness by about 10^{-3} lasted about 4.4 days, and the detailed light curve can be explained by the transit of a string of half a dozen of exocomets with a typical dust production rate of 10^5 to 10^6 kg s^{-1} [48].

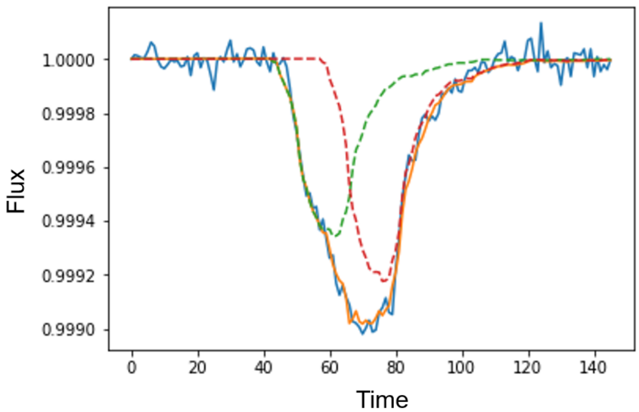

Figure 3. Plot of the KIC 3542116 light curve with a transit of an exocomet (blue line). The light curve can be fitted by the transit of two cometary nuclei on the same orbit with a periastron located at 1 au from the star, a longitude of periastron of -45° and dust production rates of 7 10^6 and 9 10^6 kg s^{-1} (green and red dotted lines).
(courtesy of L. Cros)

With an extensive search of exocomet transit signatures in the whole data set of the Kepler light curves (about 150 000 stars), six exocomet transits have been detected in front of the star KIC 3542116 and one transit in front of the star KIC 11084727 [49]. Three of the transits in KIC 3542116 are deeper transits with star brightness decrease of about 10^{-3} that last for about a day, and three are shallower and of shorter duration. All the observed light curves of these seven

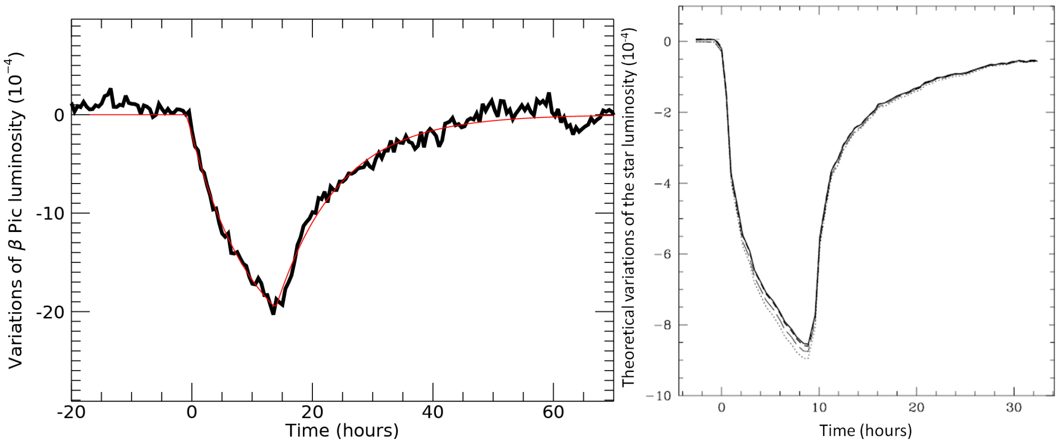

Figure 4. Light curves of an exocomet transit, as predicted and observed for β Pictoris.
The left plot shows the light curve of β Pictoris observed with TESS during the transit of an exocomet in front of this star on January 2, 2019 [51–53].
The right plot shows the theoretical light curve of an exocomet transit predicted more than 20 years ago by Lecavelier des Etangs et al. [46].

photometric events detected with Kepler are consistent with the theoretical light curve predicted for exocomets transits. A detailed analysis of these light curves allowed the estimates of the dust production rate and orbital characteristics of the comets [50] (Fig. 3).

4.3. *Exocomet size distribution*

A major step forward has been made thanks to the observations of β Pictoris with the TESS satellite. Indeed, β Pictoris was not in the Kepler field of view and we had to wait for the TESS observations to have long term photometric survey of this star. The first set of observations with TESS, from October 2018 to February 2019, yields the detection of three photometric transits of exocomets [51]. The shape of the deepest transit light curve is amazingly similar to the one predicted using numerical simulations in the end of the 90's[45, 46] (Fig. 4). Therefore, there is no doubt that the detected photometric events are due to the transits of exocomets dust tails.

After this first set of TESS observations, β Pictoris has been re-observed from November 2020 to February 2021. A new analysis of the whole data set by an Ukrainian team from Kyiv Observatory allowed the detection of five new events, putting the number of photometric detection of exocomets in β Pictoris to the total of eight [52].

Using cross-correlation techniques to identify shallow transits, a deep analysis of the same TESS data set covering 156 days of observations allowed the detection of a total of 30 exocomets [53]. This is by far the largest number of photometric detections of exocomets ; this number allows statistical analysis on the exocomets properties. Indeed, one of the advantage of the photometric detections compared to the spectroscopic detections is that the photometry traces the dust content of the tail. Therefore the measurement of the transit depth provides a direct estimate of the dust production rate from the comets nuclei. Using a library of the theoretical exocomets transit light curves, the distance of the comet to the star at the time of the transit can also be estimated [53]. Using the measurements made on the well-studied Solar system dusty comet Hale-Bopp as a reference [54–56], the size of the comets' nuclei can be derived from the estimated dust production rates normalized to a distance of 1 au from the star. Finally, the 30 photometric

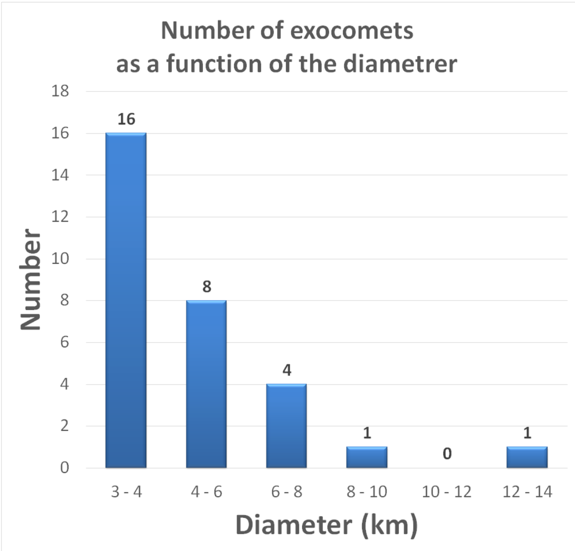

Figure 5. Histogram of the size of exocomets discovered in the β Pic planetary system. While 16 exocomets are between 3 and 4 kilometers in diameter, only 4 have a diameter between 6 and 8 kilometers and only one comet has a diameter between 8 and 10 kilometers. This rapid decrease in the number of objects for large sizes is characteristic of objects produced by collision and fragmentation.

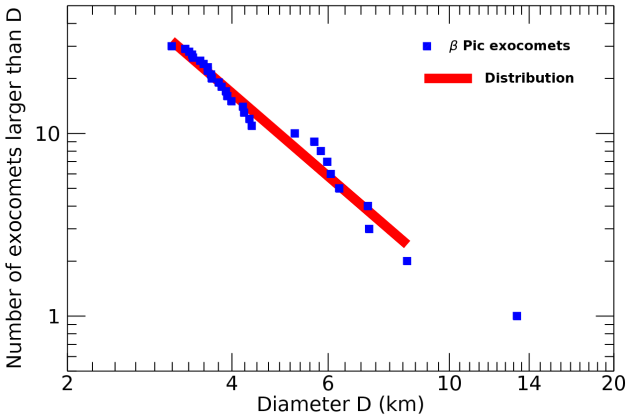

Figure 6. Distribution of the size of exocomets discovered in the β Pic planetary system. The size of each of the 30 exocomets detected with TESS photometry is shown by a blue square. The red line indicates the expected distribution for a population of objects produced by collisions.

detections of exocomets with TESS yield an estimate of the comets nuclei size distribution in the β Pictoris system (Fig. 5). The differential size distribution is found to follow a power law in the form $dN(R) \propto R^{-\gamma} dR$, where R is the comets radius and dN is the number of comets with sizes between R and $R + dR$. The statistical analysis of the 30 detections yields $\gamma = 3.6 \pm 0.8$ (Fig. 6). This distribution can be compared to the one observed in the Solar system for comets in the Jupiter family or in the Oort cloud [57, 58], where γ is always found to be close to the canonical value $\gamma_D = 3.5$ calculated by Dohnanyi for a collisionally relaxed population [59]. In conclusion, the statistical analysis of the observed photometric transits shows that the collisional process with fragmentation cascades is likely one of the dominant processes that shape the population of kilometer-sized bodies in the β Pictoris planetary system [53].

5. Conclusion

Finally, the large amount of observations of exocomets transits allowed to draw a detailed picture of planetary systems, where these small bodies are full members of planetary systems together with the interplanetary gas and dust, asteroids and planets. Still, new challenges arise for the next decades. Upcoming observations with new generations of telescopes like the ELTs or space observatories like the JWST will allow to address important questions. For instance, the chemical, physical and orbital characteristics need to be better constrained for a larger number of planetary systems. As an example, by the combination of spectroscopic and photometric observations, access to the gas to dust ratio will allow to have a better view on the formation history, and to be compared with what we know for the Solar system.

The interaction of exocomets with the other components of the planetary systems will be investigated: with the debris disks in the young systems and with the massive planets everywhere. Comets are not only beautiful objects enlightening the night sky, they are the messengers of the planetary systems life.

Conflicts of interest

The author has no conflict of interest to declare.

References

[1] D. Charbonneau, T. M. Brown, R. W. Noyes, R. L. Gilliland, "Detection of an Extrasolar Planet Atmosphere", *Astrophys. J.* **568** (2002), no. 1, p. 377-384.

[2] A. Vidal-Madjar, A. Lecavelier des Étangs, J.-M. Désert *et al.*, "An extended upper atmosphere around the extrasolar planet HD209458b", *Nature* **422** (2003), no. 6928, p. 143-146.

[3] D. K. Sing, J. J. Fortney, N. Nikolov *et al.*, "A continuum from clear to cloudy hot-Jupiter exoplanets without primordial water depletion", *Nature* **529** (2016), no. 7584, p. 59-62.

[4] T. M. Evans, D. K. Sing, T. Kataria *et al.*, "An ultrahot gas-giant exoplanet with a stratosphere", *Nature* **548** (2017), no. 7665, p. 58-61.

[5] B. Benneke, I. Wong, C. Piaulet *et al.*, "Water Vapor and Clouds on the Habitable-zone Sub-Neptune Exoplanet K2-18b", *Astrophys. J. Lett.* **887** (2019), no. 1, article no. L14.

[6] A. Tsiaras, I. P. Waldmann, G. Tinetti, J. Tennyson, S. N. Yurchenko, "Water vapour in the atmosphere of the habitable-zone eight-Earth-mass planet K2-18 b", *Nat. Astron.* **3** (2019), p. 1086-1091.

[7] B. Charnay, D. Blain, B. Bézard *et al.*, "Formation and dynamics of water clouds on temperate sub-Neptunes: the example of K2-18b", *Astron. Astrophys.* **646** (2021), article no. A171.

[8] B. Bézard, B. Charnay, D. Blain, "Methane as a dominant absorber in the habitable-zone sub-Neptune K2-18 b", *Nat. Astron.* **6** (2022), p. 537-540.

[9] A. Lecavelier des Étangs, F. Pont, A. Vidal-Madjar, D. K. Sing, "Rayleigh scattering in the transit spectrum of HD 189733b", *Astron. Astrophys.* **481** (2008), no. 2, p. L83-L86.

[10] D. K. Sing, A. Lecavelier des Étangs, J. J. Fortney *et al.*, "HST hot-Jupiter transmission spectral survey: evidence for aerosols and lack of TiO in the atmosphere of WASP-12b", *Mon. Not. Roy. Astron. Soc.* **436** (2013), no. 4, p. 2956-2973.

[11] A. Lecavelier des Étangs, A. Vidal-Madjar, J.-M. Désert, D. K. Sing, "Rayleigh scattering by H_2 in the extrasolar planet HD 209458b", *Astron. Astrophys.* **485** (2008), no. 3, p. 865-869.

[12] A. Vidal-Madjar, D. K. Sing, A. Lecavelier des Étangs *et al.*, "The upper atmosphere of the exoplanet HD 209458 b revealed by the sodium D lines. Temperature-pressure profile, ionization layer, and thermosphere", *Astron. Astrophys.* **527** (2011), article no. A110.

[13] C. M. Huitson, D. K. Sing, A. Vidal-Madjar *et al.*, "Temperature-pressure profile of the hot Jupiter HD 189733b from HST sodium observations: detection of upper atmospheric heating", *Mon. Not. Roy. Astron. Soc.* **422** (2012), no. 3, p. 2477-2488.

[14] D. Dragomir, B. Benneke, K. A. Pearson *et al.*, "Rayleigh Scattering in the Atmosphere of the Warm Exo-Neptune GJ 3470b", *Astrophys. J.* **814** (2015), no. 2, article no. 102.

[15] I. A. G. Snellen, B. R. Brandl, R. J. de Kok *et al.*, "Fast spin of the young extrasolar planet β Pictoris b", *Nature* **509** (2014), no. 7498, p. 63-65.

[16] M. Mayor, D. Queloz, "A Jupiter-mass companion to a solar-type star", *Nature* **378** (1995), no. 6555, p. 355-359.

[17] H. Lammer, F. Selsis, I. Ribas *et al.*, "Atmospheric Loss of Exoplanets Resulting from Stellar X-Ray and Extreme-Ultraviolet Heating", *Astrophys. J. Letters* **598** (2003), no. 2, p. L121-L124.

[18] V. Bourrier, A. Lecavelier des Étangs, "3D model of hydrogen atmospheric escape from HD 209458b and HD 189733b: radiative blow-out and stellar wind interactions", *Astron. Astrophys.* **557** (2013), article no. A124.

[19] V. Bourrier, A. Lecavelier des Étangs, "3D model of hydrogen atmospheric escape from HD 209458b and HD 189733b: radiative blow-out and stellar wind interactions", *Astron. Astrophys.* **557** (2013), article no. A124.

[20] V. Bourrier, D. Ehrenreich, A. Lecavelier des Étangs, "Radiative braking in the extended exosphere of GJ 436 b", *Astron. Astrophys.* **582** (2015), article no. A65.

[21] V. Bourrier, A. Lecavelier des Étangs, D. Ehrenreich, Y. A. Tanaka, A. A. Vidotto, "An evaporating planet in the wind: stellar wind interactions with the radiatively braked exosphere of GJ 436 b", *Astron. Astrophys.* **591** (2016), article no. A121.

[22] B. Lavie, D. Ehrenreich, V. Bourrier *et al.*, "The long egress of GJ 436b's giant exosphere", *Astron. Astrophys.* **605** (2017), article no. L7.

[23] V. Bourrier, A. Lecavelier des Étangs, D. Ehrenreich *et al.*, "Hubble PanCET: an extended upper atmosphere of neutral hydrogen around the warm Neptune GJ 3470b", *Astron. Astrophys.* **620** (2018), article no. A147.

[24] A. Lecavelier des Étangs, "A diagram to determine the evaporation status of extrasolar planets", *Astron. Astrophys.* **461** (2007), no. 3, p. 1185-1193.

[25] D. Ehrenreich, J.-M. Désert, "Mass-loss rates for transiting exoplanets", *Astron. Astrophys.* **529** (2011), article no. A136.

[26] E. D. Lopez, J. J. Fortney, N. Miller, "How Thermal Evolution and Mass-loss Sculpt Populations of Super-Earths and Sub-Neptunes: Application to the Kepler-11 System and Beyond", *Astrophys. J.* **761** (2012), no. 1, article no. 59.

[27] M. S. Lundkvist, H. Kjeldsen, S. Albrecht *et al.*, "Hot super-Earths stripped by their host stars", *Nat. Commun.* **7** (2016), article no. 11201.

[28] E. D. Lopez, J. J. Fortney, "The Role of Core Mass in Controlling Evaporation: The Kepler Radius Distribution and the Kepler-36 Density Dichotomy", *Astrophys. J.* **776** (2013), no. 1, article no. 2.

[29] R. Ferlet, L. M. Hobbs, A. Vidal-Madjar, "The beta Pictoris circumstellar disk. V. Time variations of the Ca II-K line", *Astron. Astrophys.* **185** (1987), p. 267-270.

[30] H. Beust, A.-M. Lagrange-Henri, A. Vidal-Madjar, R. Ferlet, "The beta Pictoris circumstellar disk. X. Numerical simulations of infalling evaporating bodies", *Astron. Astrophys.* **236** (1990), p. 202-216.

[31] H. Beust, A.-M. Lagrange, F. Plazy, D. Mouillet, "The β Pictoris circumstellar disk. XXII. Investigating the model of multiple cometary infalls", *Astron. Astrophys.* **310** (1996), p. 181-198.

[32] A. Vidal-Madjar, A.-M. Lagrange-Henri, P. D. Feldman *et al.*, "HST-GHRS observations of β Pictoris: additional evidence for infalling comets", *Astron. Astrophys.* **290** (1994), p. 245-258.

[33] A. Vidal-Madjar, A. Lecavelier des Étangs, R. Ferlet, "β Pictoris, a young planetary system? A review", *Planet. Space Sci.* **46** (1998), no. 6, p. 629-648.

[34] F. Kiefer, A. Lecavelier des Étangs, J. Boissier *et al.*, "Two families of exocomets in the β Pictoris system", *Nature* **514** (2014), no. 7523, p. 462-464.

[35] F. Kiefer, A. Lecavelier des Étangs, J.-C. Augereau *et al.*, "Exocomets in the circumstellar gas disk of HD 172555", *Astron. Astrophys.* **561** (2014), article no. L10.

[36] C. A. Grady, A. Brown, B. Y. Welsh, A. Roberge, I. Kamp, P. Rivière Marichalar, "The Star-grazing Bodies in the HD 172555 System", *Astron. J.* **155** (2018), no. 6, article no. 242.

[37] S. L. Montgomery, B. Y. Welsh, "Detection of Variable Gaseous Absorption Features in the Debris Disks Around Young A-type Stars", *Publ. Astron. Soc. Pac.* **124** (2012), no. 920, p. 1042-1056.

[38] A. Roberge, B. Y. Welsh, I. Kamp, A. J. Weinberger, C. A. Grady, "Volatile-rich Circumstellar Gas in the Unusual 49 Ceti Debris Disk", *Astrophys. J. Letters* **796** (2014), no. 1, article no. L11.

[39] B. E. Miles, A. Roberge, B. Y. Welsh, "UV Spectroscopy of Star-grazing Comets Within the 49 Ceti Debris Disk", *Astrophys. J.* **824** (2016), no. 2, article no. 126.

[40] A.-M. Lagrange-Henri, H. Beust, R. Ferlet, L. M. Hobbs, A. Vidal-Madjar, "HR 10 : a new beta Pictoris-like star ?", *Astron. Astrophys.* **227** (1990), p. L13-L16.

[41] A. Lecavelier des Étangs, A. Vidal-Madjar, D. E. Backman *et al.*, "Discovery of CI around 51 Ophiuchi", *Astron. Astrophys.* **321** (1997), p. L39-L42.

[42] A. Lecavelier des Étangs, M. Deleuil, A. Vidal-Madjar *et al.*, "HST-GHRS observations of candidate β Pictoris-like circumstellar gaseous disks", *Astron. Astrophys.* **325** (1997), p. 228-236.

[43] I. Rebollido, C. Eiroa, B. Montesinos *et al.*, "Exocomets: A spectroscopic survey", *Astron. Astrophys.* **639** (2020), article no. A11.

[44] B. Y. Welsh, S. L. Montgomery, "Circumstellar Gas-Disk Variability Around A-Type Stars: The Detection of Exocomets?", *Publ. Astron. Soc. Pac.* **125** (2013), no. 929, p. 759-774.
[45] A. Lecavelier des Étangs, "A library of stellar light variations due to extra-solar comets", *Astron. Astrophys. Suppl. Ser.* **140** (1999), p. 15-20.
[46] A. Lecavelier des Étangs, A. Vidal-Madjar, R. Ferlet, "Photometric stellar variation due to extra-solar comets", *Astron. Astrophys.* **343** (1999), p. 916-922.
[47] T. S. Boyajian, D. M. LaCourse, S. A. Rappaport *et al.*, "Planet Hunters IX. KIC 8462852 - where's the flux?", *Mon. Not. Roy. Astron. Soc.* **457** (2016), no. 4, p. 3988-4004.
[48] F. Kiefer, A. Lecavelier des Étangs, A. Vidal-Madjar *et al.*, "Detection of a repeated transit signature in the light curve of the enigma star KIC 8462852: A possible 928-day period", *Astron. Astrophys.* **608** (2017), article no. A132.
[49] S. A. Rappaport, A. Vanderburg, T. Jacobs *et al.*, "Likely transiting exocomets detected by Kepler", *Mon. Not. Roy. Astron. Soc.* **474** (2018), no. 2, p. 1453-1468.
[50] A. Lecavelier des Étangs, L. Cros *et al.*, in preparation, 2022.
[51] S. Zieba, K. Zwintz, M. A. Kenworthy, G. M. Kennedy, "Transiting exocomets detected in broadband light by TESS in the β Pictoris system", *Astron. Astrophys.* **625** (2019), article no. L13.
[52] Y. Pavlenko, I. Kulyk, O. Shubina *et al.*, "New exocomets of β Pic", *Astron. Astrophys.* **660** (2022), article no. A49.
[53] A. Lecavelier des Etangs, L. Cros, G. Hébrard *et al.*, "Exocomets size distribution in the β? Pictoris planetary system", *Sci. Rep.* **12** (2022), article no. 5855.
[54] D. Jewitt, H. Matthews, "Particulate Mass Loss from Comet Hale-Bopp", *Astron. J.* **117** (1999), no. 2, p. 1056-1062.
[55] Y. R. Fernández, D. D. Wellnitz, M. W. Buie *et al.*, "The Inner Coma and Nucleus of Comet Hale-Bopp: Results from a Stellar Occultation", *Icarus* **140** (1999), no. 1, p. 205-220.
[56] A. N. Bair, D. G. Schleicher, T. Farnham, "The Extremely Active Comet C/Hale-Bopp (1995 O1): Production Rates from Nearly Five Years of Narrowband Photometry", in *AAS/Division for Planetary Sciences Meeting Abstracts #50*, AAS/Division for Planetary Sciences Meeting Abstracts, vol. 50, 2018.
[57] J. M. Bauer, T. Grav, Y. R. Fernández *et al.*, "Debiasing the NEOWISE Cryogenic Mission Comet Populations", *Astron. J.* **154** (2017), no. 2, article no. 53.
[58] B. Boe, R. Jedicke, K. J. Meech *et al.*, "The orbit and size-frequency distribution of long period comets observed by Pan-STARRS1", *Icarus* **333** (2019), p. 252-272.
[59] J. S. Dohnanyi, "Collisional Model of Asteroids and Their Debris", *J. Geophys. Res.* **74** (1969), p. 2531-2554.